Shell-model description of the β^- decay of the $N=21$ and 22 isotones ^{34}Al, ^{36}Si, and ^{37}P

E. K. Warburton
Brookhaven National Laboratory, Upton, New York 11973

J. A. Becker
Lawrence Livermore National Laboratory, Livermore, California 94550

(Received 24 July 1987)

The nuclear structure of the parent and daughter nuclei in the decays ^{34}Al(β^-)^{34}Si, ^{36}Si(β^-)^{36}P, and ^{37}P(β^-)^{37}S are considered in a spherical shell model comprising the $(2s,1d,1f,2p)$ configuration space. Energy spectra and beta and gamma transition strengths are calculated. These predictions are used to construct decay schemes from recent β^--delayed γ-ray singles spectra for the three decaying nuclei. The predicted half-lives of ^{34}Al, ^{36}Si, and ^{37}P are 0.037(7), 0.8(4), and 2.0(9) s, where the uncertainties are due to mass uncertainties of the decaying bodies. These predictions are in agreement with recent experimental results of 0.050(25), 0.54(15), and 2.31(13) s, respectively.

I. INTRODUCTION

The formation of very neutron-rich light ($A \lesssim 40$) nuclei and the investigation of their decays is an area of research of considerable current interest and activity. Experimental techniques and apparatus have been greatly improved in recent years, as for example at the GANIL (Grand Accélérateur National d'Ions Lourds, Caën, France) intermediate energy heavy-ion facility.[1,2] The spectroscopy of these exotic nuclei is especially revealing of the underlying nuclear structure.[3]

The shell-model predictions presented here for the β^- decay of ^{34}Al, ^{36}Si, and ^{37}P are a continuation of an investigation into the structure of the neutron-rich nuclei in the $A \lesssim 40$ region.[4-6] This study utilizes a spherical shell-model interaction designed to describe nuclear levels in the $A \sim 40$ region for which the nucleons occupy the seven subshells of the (sd) and (fp) major shells. The dimensions of the matrices involved increase dramatically with the number of nucleons allowed in the (fp) shell and also as $N-Z$ decreases. Thus in our first efforts we have concentrated on the simplest of these nuclei, namely $N=21$ and 22 isotones with $Z<20$.

We recently presented results for the decays of the $N=21$ isotones ^{35}Si and ^{36}P (Ref. 5). The experimental results for these nuclei were obtained at the GANIL facility by Dufour *et al.*,[2] who also reported decay information for eleven other $A<40$ nuclei. Of these, there is one other $N=21$ isotone, ^{34}Al, and two $N=22$ nuclei, ^{36}Si and ^{37}P. The spectroscopy of these decays is a logical next step in our overall study. Our calculational procedures are described in the next section and results for these three decays are presented in Sec. III.

II. CALCULATION

The shell-model interaction, designated as WBMB, has evolved somewhat from that used previously.[4-6] It still utilizes an inert ^{16}O core, the Wildenthal[7,8] "universal" $2s,1d$ (USD) interaction for the (sd) shell, and a modified Millener-Kurath[9] (sd) to (fp) cross-shell interaction. One change is to adopt the McGrory[10] interaction to describe the (fp) shell. This results in a much better description of the $A=42-44$ Ca and Sc isotopes. The other modification consists of new procedures for joining these three interactions. Briefly, the two-body matrix elements (2BME's) of the USD interaction have an A dependence of $A^{-0.3}$ and we adopt the same dependence for the Millener-Kurath and McCrory interactions for the $A<40$ nuclei of interest here. One further refinement which was found to give better agreement with experimental binding energies is made. Namely, in calculations within a $(2s,1d)^{A-16-n}(fp)^n$ model space, the 2BME of the USD are given an A dependence appropriate to $A-n$ rather than A.

The relative values of the single-particle energies (SPE) of the $(2s,1d)$ and $(1f,2p)$ orbits are set at the appropriate values of the USD and McGrory interactions. All that remains to be determined is the energy gap, $\Delta(df)$, between the $(2s,1d)$ and $(1f,2p)$ shells.

For all three interactions, the (SPE) are taken to be mass independent. For the USD interaction, the constancy of the SPE follows since all A dependence is confined to the 2BME in the least-squares fit to binding energies which yields the interaction. The cross-shell interaction is generated from a potential with some adjustment of crucial $d_{3/2}$-$f_{7/2}$ and $d_{3/2}$-$p_{3/2}$ 2BME in order to fit better the $A=40$ 1p-1h spectra. The energy gap $\Delta(df)$ is set for best reproduction of $A=35-41$ binding energies for states with one or two nucleons in the fp shell. In doing so we note no significant improvement in the root-mean-square deviation from experiment if $\Delta(df)$ is allowed to vary linearly with A.

Computation in this and the previous work was carried out with the shell-model code[11] OXBASH which is formulated in the m scheme. Our calculations will be performed in the model spaces $(sd)^{A-16-n}(fp)^n$ with $n=0$, 1, or 2. We shall refer to states in these spaces as nfp states. Some of the desired calculations involve dimensions which exceed our computer resources, specifically the available disk space. Dimensions relevant to the present study are collected in Table I. The J dimension $D(J)$ is most critical since a $D(J)\cdot D(J)$ matrix must be diagonalized. The m dimension, $D(m)$, also can be a

TABLE I. Dimensions of $1fp$ and $2fp$ model spaces for $A=34-37$ nuclei. The truncations T-A and T-B are explained in the text as is the significance of the dimensions. For each model space the dimensions are given only for the J (of those considered) for which they are maximum.

	J^π,T	Model space	J dimension	m dimension
^{34}Al	$3^-,4$	$1fp$ (full)	380	922
^{34}Si	$3^-,3$	$1fp$ (full)	4431	19 105
^{35}Si	$7/2^-,7/2$	$1fp$ (full)	424	1299
^{35}P	$7/2^-,5/2$	$1fp$ (full)	3808	14 674
^{36}Si	$0^+,4$	$2fp$ (full)	718	19 354
^{36}P	$2^-,3$	$1fp$ (full)	353	1655
	$1^+,3$	$2fp$ (full)	18 870	227 478
	$1^+,3$	$2fp$ (T-A)	3310	42 606
	$1^+,3$	$2fp$ (T-B)	1841	24 304
^{37}P	$1/2^+,7/2$	$2fp$ (full)	1173	16 539
^{37}S	$3/2^-,5/2$	$1fp$ (full)	210	1149
	$3/2^+,5/2$	$2fp$ (full)	16 197	143 727
	$3/2^+,5/2$	$2fp$ (T-A)	3418	32 327
	$3/2^+,5/2$	$2fp$ (T-B)	1944	17 266

limiting factor since it enters as $D(J)\cdot D(m)$ in the projection of basis vectors with good J and T. It is the $2fp$ calculations for ^{36}P and ^{37}S which cannot be performed in the full WBMB space. The calculations for the $2fp$ states of ^{36}Si and ^{37}P and the $1fp$ states of ^{36}P and ^{37}S are well within our capabilities, while the matrices involved in the calculation for the $1fp$ states of ^{34}Si are the largest we have successfully diagonalized.

In OXBASH, truncation is accomplished by selection of partitions; a partition being a specific occupancy of the subshells included in the model space. In the present case we designate the partitions as

$$[n(d_{5/2}),n(d_{3/2}),n(s_{1/2})\,;\; n(f_{7/2}),n(f_{5/2}),n(p_{3/2}),n(p_{1/2})]$$

where $n(j)$ is the occupancy of the subshell j. In an examination of the effects of truncation, many different truncation schemes were tried. We were challenged to obtain the closest approximation possible to a full $(2s,1d,1f,2p)$ calculation for the specific purpose of calculating allowed Gamow-Teller (GT) beta decay. The truncation T-A of Table I gives dimensions which are just within the available computer resources for the ^{37}S $1/2^+$, $3/2^+$ levels and the ^{36}P 1^+ levels, and thus could be used for the calculation of the GT beta decays. In order to handle $3/2<J<9/2$ in ^{37}P and $1<J<6$ in ^{36}P it was necessary to truncate further to the scheme T-B. For ^{36}P, the scheme T-A is composed of the 87 partitions belonging to the sets:

$$[8-9,\le 8,\le 4;2,0,0,0]+[10-11,\le 8,\le 4;\le 2,0,\le 2,0]+[12,\le 8,\le 4;\le 2,\le 2,\le 2,\le 2]\ . \quad (1)$$

For ^{37}S, the $n(d_{5/2})=8$ partitions were omitted. The scheme T-B restricted the $n(d_{5/2})=10$ partitions to $n(f_{7/2})=2$, i.e., the same as for the first term of Eq. (1).

It is instructive to consider the partition composition of the wave functions generated by the calculation in scheme T-A. We list the results for ^{36}P $J^\pi=1_1^+$ in Table II: these are representative of the first few 1^+ states for ^{36}P and the first few $1/2^+$ and $3/2^+$ states of ^{37}S. Consideration of Table II illustrates why truncation of the fp shell as a function of $n(d_{5/2})$ is successful. The results suggest that $<1\%$ of the total WBMB wave function is omitted by the truncation T-A in spite of the fact that it has a J dimension $\sim\frac{1}{6}$ of that for the full WBMB space. Indeed, calculations for higher isospin states (in ^{36}Si, ^{37}P, and ^{38}S) and high-spin states in ^{36}P and ^{37}S, carried out in both full and truncated basis, support this observation. These comparison calculations also present a means of estimating the effect of the truncation on the predicted binding energies. From a comparison of predicted binding energies for 31 states in $A=36-38$ nuclei, we find that the scheme T-A underbinds by 200 ± 100 keV, where the uncertainty is one standard deviation. This comparison indicates a satisfactorily small state dependence for the binding energy shift. The pre-

TABLE II. Composition of the ^{36}P $J^\pi=1_1^+$ wave function in truncation scheme T-A.

Partition group	Intensity (%)
$[8,\le 8,\le 4;\ 2,0,0,0]$	0.2
$[9,\le 8,\le 4;\ 2,0,0,0]$	1.5
$[10,\le 8,\le 4;\ 2,0,0,0]$	9.1
$[10,\le 8,\le 4;0-1,0,1-2,0]$	0.4
$[11,\le 8,\le 4;\ 2,0,0,0]$	17.0
$[11,\le 8,\le 4;\ 0-1,0,1-2,0]$	1.5
$[12,\le 8,\le 4;\ 2,0,0,0]$	61.3
$[12,\le 8,\le 4;\ 0-1,0,1-2,0]$	6.5
$n(d_{5/2})=12;\ n(f_{5/2})+n(p_{1/2})>0$	2.5

dictions of scheme T-A were accordingly shifted by 200 keV. Similar comparison of the results from truncation scheme T-B showed that the binding energy shift associated with its use was also relatively state independent. Thus, a similar shift of 340 keV was made for the results of truncation scheme T-B. Truncation of the full WBMB model space will introduce some spuriousity. In OXBASH, spuriousity is routinely eliminated by the method of Gloeckner and Lawson.[12] This method is *approximate* so that our results do contain some spuriousity; however, since the truncation eliminates $<1\%$ of the wave functions, it seems reasonable that the spuriousity is limited to some fraction of $<1\%$ and is, therefore, not a serious problem. OXBASH contains standard procedures for testing for the effects of spuriousity which involve repeating the diagonalization under different conditions. Due to computer time restrictions we did this for ^{36}P only. The tests indicate completely negligible effect on the 10 lowest ^{36}P 1^+ states of either spuriousity or the method used to eliminate it.

Our procedures for calculating β and γ decay observables follow those described in our report of the decays of ^{35}Si and ^{36}P (Ref. 5). In particular, the Gamow-Teller beta-decay transition strength, B(GT), was calculated for all energetically accessible final states. This was found to demand ~ 200 final states for $^{34}\mathrm{Al}(\beta^-)^{34}\mathrm{Si}$ which has $Q(\beta^-)=16\,459$ keV and three possible final state spins, but only ~ 20 final states for $^{36}\mathrm{Si}(\beta^-)^{36}\mathrm{P}$ which has a smaller available phase space, $Q(\beta^-)=7347$ keV, and only one possible final state spin. The phase-space factor f was calculated using the Wilkinson-Macefield[13] parametrization and for each state k the half-life t_k was calculated from

$$t_k = 6166/[f \cdot B(\mathrm{GT})]_k \ . \tag{2}$$

The total half-life for allowed decays is then obtained from

$$1/t = \sum_k 1/t_k \ . \tag{3}$$

We use the effective Gamow-Teller operator described in Ref. 4; it is based on the "final fit" *sd*-shell value of Brown and Wildenthal.[14] Resulting B(GT) values are $\sim 60\%$ of B(GT) values obtained using the free nucleon Gamow-Teller operator. That is, half-lives calculated with the free nucleon GT operators would be $\sim 60\%$ of those presented here. Electromagnetic and first-forbidden beta-decay matrix elements are evaluated with harmonic oscillator radial wave functions, utilizing a length parameter $b=(41.467/\hbar\omega)^{1/2}$ fm ($\hbar\omega = 45A^{-1/3}-25A^{-2/3}$ MeV). The calculations of these observables follow the procedures described in Ref. 6.

The reliability of the calculations. Our experience to date with the WBMB interaction and its predecessor, the SDPF interaction, lead us to expect that level energies will be calculated with ~ 200-keV root-mean-square deviation from experiment. We expect to predict medium-to-strong $M1$, $E2$, and $E3$ γ transitions and GT β transitions with quite high accuracy (within $\sim 40\%$ in the matrix elements).[15,16] Weak transitions are usually subject to cancellation between various contributions and thus are not normally capable of being reproduced with accuracy. We are usually satisfied if the calculated values are also weak. $E1$ transitions are always a problem because of the well-known diminution of strength for low-lying transitions at the expense of the $E1$ giant resonance, and because what would be the dominant contribution, e.g., $d_{3/2} \leftrightarrow f_{7/2}$ in the present case, is forbidden for $E1$ decays.

For GT transitions, which are our main concern, the scale of transition strengths is established by the sum rule limit

$$\sum_f B(\mathrm{GT}) = (1.26)^2 3(N_i - Z_i) \ , \tag{4}$$

which applies to β^- decays in these neutron rich nuclei. For ^{36}Si and ^{37}P decays these sums are 38 and 33, respectively. Our experience is that B(GT) values less than $\sim 50\times 10^{-3}$ (i.e., $\sim 0.1\%$ of the sum rule) cannot be predicted reliably.

III. RESULTS

A. Binding energies and energy spectra

We first compare the experimental and predicted binding energies of the *nfp* model spaces of interest. The mass excesses of ^{34}Al, ^{36}Si, and ^{37}P have recently been measured for the first time.[17] Results (nucleus: mass excess, binding energy)—with the energies in keV and the uncertainty in the last figure in parentheses—are [^{34}Al: $-3500(400)$, $-267\,756(400)$], [^{36}Si: $-12\,900(600)$, $-292\,517(600)$], [^{37}P: $-19\,310(400)$, $-306\,220(400)$]. There have been three recent measurements of the ^{34}Si mass excess.[18–20] The three, which are not in very good agreement, yield the average results: [^{34}Si: $-19\,959(24)$, $-283\,433(24)$]. The mass excess of ^{36}P has been measured by Mayer *et al.*[18] and Drumm *et al.*[21] The results of $-20\,252(15)$ keV and $-20\,251(27)$ keV are in excellent agreement, yielding the weighted averages: [^{36}P: $-20\,249(13)$, $-299\,081(13)$]. The mass excess and binding energy of ^{37}S, as reported in the mass table,[22] are [^{37}S: $-26\,896.59(26)$, $-313\,019.8(4)$].

The predicted binding energies E_{Bcorr} of the WBMB interaction do not include Coulomb contributions and they are relative to the ^{16}O core. Comparison to experiment is made by subtracting the Coulomb contribution from the experimental binding energies to yield experimental values for E_{Bcorr}. There are several possible ways of estimating the Coulomb corrections, all of which entail uncertainties of the order of 100–200 keV. We start from Wildenthal's results[8] for the lighter $Z=14$–16 isotopes and assume that the difference between the experimental binding energy and the corrected binding energy, E_{Bcorr}, is independent of A for a given Z. We adopt the average of the results obtained by extrapolation from the 3–4 next lighter isotopes. This procedure gives the experimental E_{Bcorr} of Table III. Except for ^{34}Al, the comparison of predicted and empirical E_{Bcorr} shown in Table III displays quite satisfactory agreement, and indicates

TABLE III. Experimental and predicted Coulomb corrected binding energies, E_{Bcorr}, for the lowest-lying state of each nfp model space of interest. The difference (experiment minus predicted) is also given if known.

Nucleus	State J^π	E_{Bcorr} (keV) Expt.	Pred.	Difference (keV)
^{34}Al	$4^-,5^-$	−161 650(400)	−161 088	−562(400)
^{34}Si	0^+	−182 594(24)	−182 747	+153(24)
^{34}Si	4^-		−178 520	
^{36}Si	0^+	−191 753(600)	−191 948	+185(600)
^{36}P	4^-	−204 074(13)	−204 410	+336(13)
^{36}P	1^+	−202 771(13)	−203 206	+435(13)
^{37}P	$1/2^+$	−211 079(400)	−211 474	+395(400)
^{37}S	$7/2^-$	−223 872(1)	−224 043	+171(1)
^{37}S	$3/2^+$	−222 477(1)	−222 444	−33(1)

that the WBMB interaction has useful predictive powers for binding energies at least for $A > 34$. For ^{34}Al we appear to be seeing the onset of deformation which is known to occur for $N \simeq 20$, $A \sim 30$–33 nuclei.[3] If so, proper account of the binding energy of ^{34}Al would necessitate inclusion of $> 1\hbar\omega$ terms in the wave functions. The WBMB predictions for the $1fp$ spectrum of ^{34}Al and the $2fp$ spectra of ^{36}Si and ^{37}P are listed in Table IV. As discussed, these were calculated within a full WBMB basis. There is no known experimental information on the spectra of any of these three nuclei.

The WBMB predictions for the $(0-1)fp$ spectrum of ^{34}Si and the $(1-2)fp$ spectra of ^{36}P and ^{37}S are listed in Table V. The ^{34}Si spectrum and the $1fp$ spectrum of ^{36}P and ^{37}S are for the full WBMB space; the results for the $2fp$ spectra of ^{36}P and ^{37}S are from truncation scheme T-B, with all excitation energies shifted downwards by 340 keV as explained in Sec. II.

^{34}Si excited states. Both Mayer *et al.*[18] and Fifield *et al.*[19] used two-proton pickup reactions on ^{36}S to form ^{34}Si. Mayer *et al.*[18] reported one excited state at 3590(25) keV, which, however, Fifield *et al.*[19] did not observe. The reactions used in the two investigations are similar enough so that this is a real discrepancy, and therefore the existence of this excited state must be viewed as questionable. Fifield *et al.*[19] observed an excited state at 5330(50) keV. They present arguments associating this state with the 2_1^+ state predicted to lie at 4888 keV (Table V). As noted by Fifield *et al.*,[19] two proton pickup would not be expected to form the $1fp$ states with observable cross sections.

A question of interest is at what excitation energy the $2\hbar\omega$ $2fp$ states will commence. The $(2s,1d)^{16}(fp)^2$ space is too large for us to treat without truncation. Therefore, calculations were performed in several truncation schemes in order to estimate this energy. The results indicate that the $2fp$ states start with a 0^+ state at $\sim$7-MeV excitation with a 2^+ state $\sim$1.5 MeV higher. A calculation in the mixed $(0+2)fp$ space was also made using the van der Poel interaction which uses the truncated $(s_{1/2},d_{3/2},f_{7/2},p_{3/2})$ configurational space.[23] This calculation gave $\sim$4 MeV for the excitation of 0_2^+ in ^{34}Si. In either case, the excitation energy of the first $2fp$ 2^+ state would be too high to have any influence on the present results, i.e., too high to be formed significantly either directly or indirectly by β^- decay from ^{34}Si.

^{36}P excited states. Prior to the beta-decay results of Dufour *et al.*,[2] energy levels were reported in ^{36}P at 252(10) keV (Ref. 21) and 450(22) keV (Ref. 18) from heavy-ion transfer results. The ^{36}Si β^- decay results of Ref. 2 suggest levels below 1300-keV excitation at 250.25(40) and 424.90(40) keV in agreement with the transfer results and in satisfactory agreement with our predictions (Table V) for the lowest 4^-, 3^-, and 2^- levels. We have previously presented evidence from an analysis[5] of the ^{36}P$(\beta^-)^{36}$S results of Dufour *et al.*,[2] which supports an assignment of 4^- to the ^{36}P ground state.

^{37}S excited states. Prior to the ^{37}P$(\beta^-)^{37}$S results of Dufour *et al.*,[2] information on the energy spectrum of ^{37}S has come mainly from the ^{36}S(d,p)^{37}S reaction,[24,25] the ^{36}S(n,γ)^{37}S reaction,[26] and the ^{37}Cl(t,^{3}He)^{37}S reaction.[27] Only one definite and one probable even-parity state were identified, and we will find, not surprisingly, that new ^{37}S states are involved in the allowed beta decay of $J^\pi = 1/2^+$ ^{37}P.

Our main concern at this point is to attempt an identification of the lowest-lying odd-parity intruder states, i.e., those arising from nfp excitations with $n > 1$ and therefore outside our model space. The WBMB predictions for the single-neutron spectroscopic factors of $^{36}\text{S} + \text{n} \rightarrow {}^{37}\text{S}$ are listed in Table VI for the first five $J = 1/2-7/2$ $1fp$ states of ^{37}S. The predicted stripping strength is concentrated in the first two $7/2^-$ and $3/2^-$ states and the first $1/2^-$ state. For $J^\pi = 5/2^-$, the strength is predicted to be more widely fragmented with the centroid at $\sim$5-MeV excitation. These results are consistent with the previous predictions of Woods,[28] who performed calculations for ^{37}S in a $(1d_{5/2},1d_{3/2},2s_{1/2},1f_{7/2},2p_{3/2})$ model space and thus presented S_n^+ factors for $7/2^-$ and $3/2^-$ states (but not for $1/2^-$ or $5/2^-$ states). The predictions are compared to experiment in Table VII and Fig. 1 with the purpose of identifying intruder states: That there are low-lying intruder states is evident from the comparison of Fig. 1. There are seven experimental levels below 4-MeV excita-

TABLE IV. The predicted $1fp$ spectra of ^{34}Al and $2fp$ spectra of ^{36}Si and ^{37}P. No. orders the states of a given J^π by energy. All states are listed up to the first No. equal to 8, after that only yrast (i.e., No equal to 1) states are listed.

^{34}Al			^{36}Si			^{37}P		
E_x (keV)	J^π	No.	E_x (keV)	J^π	No.	E_x (keV)	J^π	No.
0000	5^-	1	0000	0^+	1	0000	$1/2^+$	1
0002	4^-	1	1898	2^+	1	1480	$3/2^+$	1
0476	3^-	1	3074	4^+	1	1753	$5/2^+$	1
0515	6^-	1	4022	2^+	2	2506	$3/2^+$	2
0757	2^-	1	4022	6^+	1	2817	$9/2^+$	1
1502	3^-	2	4936	4^+	2	2914	$7/2^+$	1
1769	4^-	2	5034	3^+	1	3416	$5/2^+$	2
1848	2^-	2	5055	0^+	2	3672	$3/2^+$	3
2544	1^-	1	5085	2^+	3	3770	$13/2^+$	1
3124	2^-	3	5428	5^+	1	3876	$11/2^+$	1
3151	3^-	3	5761	3^+	2	4031	$5/2^+$	3
3295	4^-	3	6055	2^+	4	4112	$7/2^+$	2
3371	3^-	4	6275	4^+	3	4292	$9/2^+$	2
3509	2^-	4	6372	3^+	3	4321	$5/2^+$	4
3908	5^-	2	6450	0^+	3	4328	$1/2^+$	2
3909	1^-	2	6500	4^+	4	4581	$1/2^+$	3
4129	1^-	3	6611	3^+	4	4633	$7/2^+$	3
4216	0^-	1	6846	4^+	5	4686	$11/2^+$	2
4498	3^-	5	7096	1^+	1	4830	$7/2^+$	4
4521	2^-	5	7289	2^+	5	4923	$3/2^+$	4
4524	4^-	4	7395	6^+	2	4929	$5/2^+$	5
4801	7^-	1	7402	5^+	2	5000	$5/2^+$	6
4843	2^-	6	7481	2^+	6	5204	$9/2^+$	3
4849	6^-	2	7562	2^+	7	5455	$9/2^+$	4
4884	5^-	3	7574	5^+	3	5535	$11/2^+$	3
4896	6^-	3	7787	6^+	3	5546	$5/2^+$	7
4954	1^-	4	7884	3^+	5	5606	$3/2^+$	5
4991	3^-	6	7909	1^+	2	5619	$7/2^+$	5
5139	4^-	5	8005	2^+	8	5674	$9/2^+$	5
5359	0^-	2	8371	7^+	1	5798	$7/2^+$	6
5416	4^-	6	8905	8^+	1	5868	$9/2^+$	6
5494	2^-	7	9921	9^+	1	5895	$15/2^+$	1
5498	5^-	4	11467	10^+	1	6025	$7/2^+$	7
5509	1^-	5	15895	11^+	1	6092	$9/2^+$	7
5604	5^-	5	16814	12^+	1	6216	$5/2^+$	8
5642	6^-	4	24117	13^+	1	8139	$17/2^+$	1
5647	3^-	7				10480	$19/2^+$	1
5720	2^-	8				11199	$21/2^+$	1
6239	8^-	1				15009	$23/2^+$	1
7720	9^-	1				18982	$25/2^+$	1
12899	10^-	1						

tion with $l_n=1$ assignments, but the WBMB interaction predicts only three $1/2^-$ or $3/2^-$ states below 4.5 MeV. We have made two estimates of the excitation energies of intruder states. The first, described in Ref. 25, uses the Bansel-French weak coupling model[29] and is labeled BF in Fig. 1. The second is a shell-model calculation with the WDF interaction[30] in a $(d_{3/2}f_{7/2})^5$ model space. The results are labeled WDF in Fig. 1. Both predict that odd-parity intruder states will start at $E_x=\sim 2$ MeV, but the order of the levels is not at all certain. Based on a scrutiny of the spectroscopic factors of Tables VI and VII and Fig. 1, we would identify the 1992-, 2023-, and 2517-keV levels as intruders. Certainly, this identification results in a much better overall agreement of predictions and experiment of the $(2J+1)S_n^+$ than would be the case for no assumed intruders. Based on the ^{36}S(n,γ)^{37}S results (Ref. 26) and ^{36}S(d,p)^{37}S results, as reviewed in Ref. 25, these states would most likely have $J^\pi=3/2^-$, $5/2^-$, and $7/2^-$, respectively. This bandlike sequence is similar to systematics of intruder states in heavier odd-A nfp nuclei (see Table V of Ref. 6). Note, however, that comparison of the predicted and experimental S_n^+ values suggests some mixing of the $1fp$ and intruder states.

TABLE V. The predicted $(0-1)fp$ spectrum of ^{34}Si and $(1-2)fp$ spectra of ^{36}P and ^{37}S. No. orders the states of a given J^π by energy. All states are listed up to the first No. equal to 6, after that only yrast (i.e., No equal to 1) states are listed.

^{34}Si			^{36}P			^{37}S		
E_x (keV)	J^π	No.	E_x (keV)	J^π	No.	E_x (keV)	J^π	No.
0000	0^+	1	0000	4^-	1	0000	$7/2^-$	1
4227	4^-	1	0169	3^-	1	0691	$3/2^-$	1
4465	3^-	1	0765	2^-	1	1599	$3/2^+$	1
4558	5^-	1	1204	1^+	1	2660	$5/2^-$	1
4888	2^+	1	1486	2^+	1	2720	$1/2^+$	1
5142	3^-	2	1540	1^-	1	3042	$7/2^+$	1
5296	2^-	1	2112	2^-	2	3114	$5/2^+$	1
5648	3^-	3	2212	0^+	1	3349	$7/2^-$	2
5999	3^+	1	2305	5^-	1	3575	$1/2^+$	2
6117	2^-	2	2403	0^-	1	3615	$3/2^+$	2
6143	4^-	2	2425	1^+	2	3635	$9/2^-$	1
6238	1^-	1	2464	2^+	2	3821	$5/2^-$	2
6426	1^-	2	2593	4^+	1	3889	$3/2^+$	3
6623	0^-	1	2649	1^-	2	3945	$5/2^+$	2
7135	1^-	3	2658	3^+	1	4109	$9/2^+$	1
7526	2^-	3	2713	3^-	2	4126	$7/2^-$	3
7600	0^+	2	3001	3^+	2	4127	$11/2^+$	1
7686	2^-	4	3140	1^+	3	4228	$9/2^-$	2
7932	4^+	1	3190	4^-	2	4273	$7/2^+$	2
8058	5^-	2	3451	2^+	3	4419	$7/2^+$	3
8128	6^-	1	3482	1^+	4	4475	$5/2^+$	3
8333	2^-	5	3545	2^+	4	4501	$3/2^+$	4
8370	4^-	3	3567	0^+	2	4583	$5/2^+$	4
8467	2^+	2	3650	3^+	3	4583	$3/2^+$	3
8536	0^-	2	3838	1^+	5	4671	$13/2^+$	1
8555	1^-	4	3845	4^+	2	4694	$3/2^+$	5
8590	3^-	4	4028	2^+	5	4701	$7/2^-$	4
8590	5^-	3	4034	0^-	2	4717	$1/2^-$	2
8732	3^-	5	4043	5^-	2	4785	$5/2^-$	3
8804	3^+	2	4045	5^+	1	4820	$3/2^+$	6
8822	3^-	6	4074	6^+	1	5171	$15/2^+$	1
10041	8^-	1	4120	4^-	3	7062	$17/2^+$	1
10142	1^+	1	4124	2^+	6	7338	$13/2^-$	1
11676	9^-	1	4443	6^-	1	7534	$15/2^-$	1
12659	5^+	1	4754	7^+	1	7909	$19/2^+$	1
13835	6^+	1	5212	8^+	1	11368	$21/2^+$	1
16044	10^-	1	7093	7^-	1	11368	$17/2^-$	1
17539	11^-	1	7220	9^+	1	11900	$23/2^+$	1
21603	7^+	1	7689	8^-	1	15035	$19/2^-$	1
24426	12^-	1	8752	10^+	1	15200	$25/2^+$	1
32029	13^-	1	11059	11^+	1	18860	$27/2^+$	1
			11496	9^-	1	26823	$29/2^+$	1
			11896	12^+	1			
			15615	10^-	1			
			15879	13^+	1			
			19316	14^+	1			
			27201	15^+	1			

B. Beta decay

1. $^{34}Al(\beta^-)^{34}Si$

Decay of ^{34}Al to ^{34}Si was calculated using the experimental $Q(\beta^-)$ of 16459(400) keV and the ^{34}Si energy spectrum of Table V. The prediction (Table IV) for the ground-state spin of ^{34}Al is ambiguous; it could as well be $J=4$ or 5. Thus, the beta decay was calculated for both alternatives. Results for allowed transitions are given in Tables VIII and IX. First-forbidden transitions were found to be strongly inhibited due both to the high excitation energies of the $0fp$ states with $J \geq 2$ in ^{34}Si and to unusually small matrix elements. For instance, the $^{34}\mathrm{Al}(4^-) \rightarrow {}^{34}\mathrm{Si}(2^+)$ unique first-forbidden transition

TABLE VI. Predicted $(2J+1)S^+$ spectroscopic factors for the reaction ^{36}S(d,p) ^{37}S leading to $1fp$ states of ^{37}S. The first five states, ordered by energy, are listed for each J^π. Numbers in parentheses are powers of 10.

	$(2J+1)S_n^+$			
No.	$1/2^-$	$3/2^-$	$5/2^-$	$7/2^-$
1	1.94	3.43	0.05	7.28
2	1.3(−3)	0.48	0.06	0.32
3	2.5(−3)	2.0(−3)	0.92	1.1(−6)
4	2.2(−4)	3.0(−4)	3.19	1.8(−2)
5	2.0(−5)	1.2(−2)	0.19	4.2(−2)

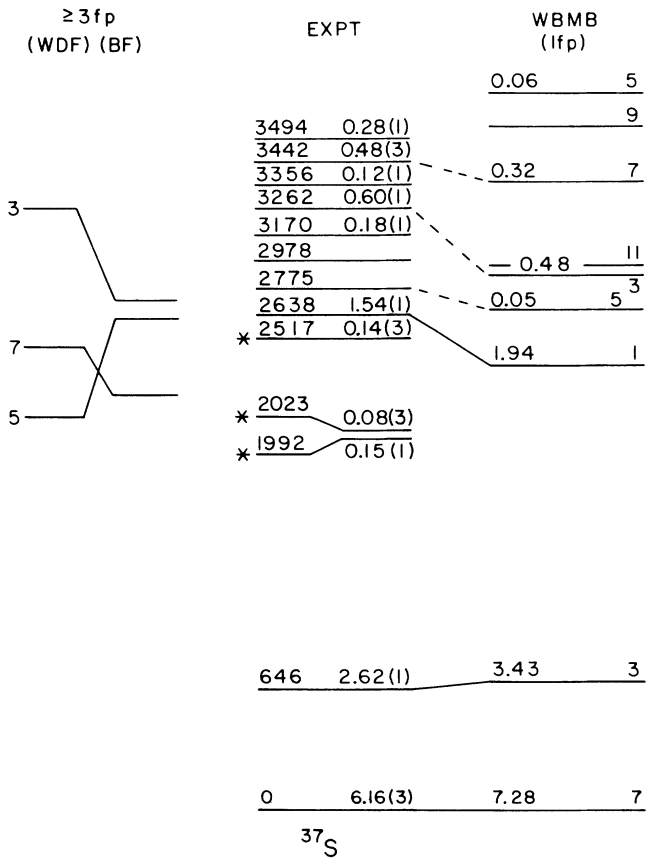

FIG. 1. Comparison of calculated and experimental properties for odd-parity (and possible odd-parity) levels of ^{37}S for $E_x < 4.0$ (expt.) and < 4.5 MeV (WBMB). The experimental spectrum is from Refs. 24 and 25, as reviewed in Ref. 25. For each level the excitation energy (in keV) is given on the left and the ^{36}S+n spectroscopic factor $(2J+1)S_n^+$ is given on the right with the associated l_n value in parentheses. For clarity, the experimental scheme between 2.9 and 3.5 MeV is not quite to scale. For the WBMB predictions,the $(2J+1)S_n^+$ are given on the left and $2J$ is on the right. Associations between experiment and the WBMB predictions are connected by solid lines if considered definite and dashed lines otherwise. The three experimental levels labeled with an asterisk are our choices for the three lowest-lying intruder ($\geq 3fp$) states. The two estimates of the $3fp$ spectra, labeled by $2J$, are for the WDF interaction and the Bansel-French weak coupling model (see text).

strength was calculated to be of order 10^{-3} relative to a $f_{7/2} \rightarrow d_{3/2}$ single-particle transition resulting in a β^- branching ratio of $\sim 1.3 \times 10^{-4}\%$.

The experimental results given by Dufour *et al.*[2] for ^{34}Al decay are very simple. One β^--delayed γ ray of 123.8(4) keV was observed, with a half-life of 0.050(25) s. The predicted half-lives for the two choices of ^{34}Al spins are coincidentally equal and are in agreement with experiment. We can understand the observation of only one low-energy γ ray if we make the reasonable assumption that the efficiency for observing high-energy γ rays was low enough so that ground-state decays from the predicted $1fp$ levels were overlooked. We note that our interaction tends to underbind the lowest 3^- state in $N \leq 20$ nuclei because it does not adequately incorporate the octupole collectivity of this state. (This is not true for $N=21$ isotones since the particle-hole interaction involved in the $1fp$ states of these nuclei is solely $T=1$ with no contribution from the $T=0$ component responsible for the aforementioned deficiency.) Then, referring to Tables VIII and IX, the observed 124-keV γ ray could correspond to a $3_1^- \rightarrow 4_1^-$ or $4_1^- \rightarrow 3_1^-$ transition (depending on the order of the 3_1^- and 4_1^- states) if $J^\pi(^{34}\text{Al})=4^-$ and either a $5_1^- \rightarrow 4_1^-$ or a $4_1^- \rightarrow 3_1^-$ transition if $J^\pi(^{34}\text{Al})=5^-$. As noted above, we expect most likely that the 3_1^- level of ^{34}Si is actually the lowest $1fp$ state so that the 124-keV γ ray corresponds to a $4_1^- \rightarrow 3_1^-$ transition. It would then seem most likely that $J^\pi(^{34}\text{Al})=4^-$, since for a 5^- assignment two observable transitions are expected; i.e., the two members of the $5_1^- \rightarrow 4_1^- \rightarrow 3_1^-$ cascade. These speculations are intended to suggest the type of experimental information needed before the ambiguity in the spin of ^{34}Al can be resolved. Two immediate studies come to mind: First, the ground-state transitions should be sought, and, second, the results of a simple timing measurement would differentiate between an $E3$ $3_1^- \rightarrow 0^+$ decay and an $M4$ $4_1^- \rightarrow 0^+$ decay. We present in Table X the predicted transition strengths connecting the lowest 0^+, 3^-, 4^-, and 5^- states of ^{34}Si. These transition strengths can be used to interpret future results on ^{34}Al$(\beta^-)^{34}$Si.

2. ^{36}Si$(\beta^-)^{36}$P

Initial results for the allowed beta decay of $J^\pi=0^+$ ^{36}Si to 1^+ states of ^{36}P were calculated using the

TABLE VII. Comparison of experimental and theoretical spectroscopic strengths for the ^{36}S(d,p)^{37}S reaction.

Experimental state			$(2J+1)S_n^+$				Model state[a]	
			Experiment		Shell model			
J^π	E_x (keV)	l_n	Ref. 25	Ref. 24	Present	Ref. 28	J_k^π	E_x (keV)
$1/2^-$	2638	1	1.54	1.66	1.94		$1/2_1^-$	2360
$3/2^-$	646	1	2.62	2.80	3.43	2.98	$3/2_1^-$	691
$(3/2)^-$	1993	1	0.15	0.30	0.48	0.90	$3/2_2^-$	2839
$3/2^-$	3261	1	0.60	0.57	0.48	0.90	$3/2_2^-$	2839
$3/2^-$	3261		0.60	0.57	2.0(−3)		$3/2_3^-$	4583
$(5/2^-,7/2^-)$	2024	(3)	0.14		0.05		$5/2_1^-$	2660
$(5/2,7/2)^-$	5499	3	1.20		3.19		$5/2_4^-$	5101
$7/2^-$	0	3	6.16	7.33	7.28	7.08	$7/2_1^-$	0
$(5/2^-,7/2^-)$	2517	(3)	0.08	0.27	0.32	0.37	$7/2_2^-$	3349
	3443	3	0.34	0.48	0.32	0.37	$7/2_2^-$	3349

[a]The subscript k orders the states of a given J^π by excitation energy.

experimental $Q(\beta^-)$ of 7347(600) keV and the ^{36}P energy spectrum of Table V. On the basis of these results, and from calculations of γ-ray transition strengths, the six β^--delayed γ rays observed by Dufour *et al.*[2] were placed in the scheme of Fig. 2. Then the β^- decay logft values and branching ratios were recalculated using the proposed two lowest energy levels of Fig. 2 together with the predicted excitation energies of the higher-lying 1^+ states. Results are given in Table XI. The two first-forbidden decays which were calculated to be the strongest are also included. These are negligible compared to the allowed decays, so that the observed β^--delayed γ-ray flux can be attributed to decays to 1^+ states only (the 0^+, $T=4$ analog of the ^{36}Si ground state is, of course, not energetically accessible).

Gamma-ray transitions. We now consider the WBMB predictions for γ-transition branching ratios since they are needed for the best interpretation of the observed β^- delayed γ rays. We first consider transitions between the $1fp$ states.

As discussed in Sec. II A, the 250- and 425-keV levels were observed previously and, assuming they have odd parity, we have the very strong prediction that the flux into the 425-keV level is from γ decay of 1^+ states populated in allowed decay. This gives us a model-dependent choice of $J^\pi=2^-$ for the 425-keV level from the $J^\pi=2^-$, 3^-, and 4^- alternatives offered by the calculation and, thus, the order of the three lowest states as shown by the dashed lines connecting the WBMB predictions to the experimental level scheme. With these proposed J^π assignments the γ-ray branching ratio of the 425-keV level seems surprising; it demands that the $2_1^-\rightarrow 4_1^-$ $E2$ transition strength be $\sim$800 times the $M1$ $2_1^-\rightarrow 3_1^-$ $M1$ strength [both expressed in Weisskopf units (W.u.)]. In actual fact these branchings are quite consistent with the WBMB predictions which are for a 11 W.u. $2_1^-\rightarrow 4_1^-$ $E2$ decay (corresponding to a partial meanlife of 0.74 ns) and an essentially vanishing $2_1^-\rightarrow 3_1^-$ $M1$ transition strength ($\sim 5\times 10^{-5}$ W.u.). Since matrix elements which are very small due to cancellation effects cannot be calculated with any accuracy, the small predicted $M1$ strength is consistent with the $\sim 10^{-3}$ W.u. needed to explain the observed branching ratio. Our predictions for the $3_1^-\rightarrow 4_1^-$ transition are for a 0.16 W.u. $M1$ decay with a meanlife of 13 ps.

As shown in Fig. 2 we have placed the observed 922-keV γ ray as feeding the 425-keV level so as to help explain the surplus flux out of the 425-keV state. Then the only candidates we have to associate with the resulting 1347-keV level are the 1_1^- or 2_1^+ model states. For the 1_1^- level possibility we predict a 0.81 W.u. $M1$ decay to 2_1^- and a 50 W.u. $E2$ decay to 3_1^-. In spite of the ex-

TABLE VIII. Predictions of ^{34}Al(β^-)^{34}Si for a ^{34}Al $J^\pi=4^-$ ground state. The predicted half-life is 0.037(7) s where the uncertainty is due to that in the mass of ^{34}Al. Only ^{34}Si states for which the branching is $>1\%$ are listed.

J_k^π	E_x (keV)	B(GT) ($\times 10^3$)	log ft	Branching (%)
4_1^-	4227	143.5	4.63	37.5
3_1^-	4465	154.1	4.60	36.7
5_1^-	4558	19.9	5.49	4.6
3_2^-	5142	29.4	5.32	5.3
3_3^-	5648	7.9	5.89	1.2
4_3^-	8370	52.8	5.07	2.0
4_4^-	8865	38.8	5.20	1.1
3_7^-	9191	51.4	5.08	1.2
3_8^-	9325	59.8	5.01	1.3

TABLE IX. Predictions of ^{34}Al(β^-)^{34}Si for a ^{34}Al $J^\pi=5^-$ ground state. The predicted half-life is 0.037(7) s where the uncertainty is due to that in the mass of ^{34}Al. Only ^{34}Si states for which the branching is $>1\%$ are listed.

J_k^π	E_x (keV)	B(GT) ($\times 10^3$)	logft	Branching (%)
4_1^-	4227	248.5	4.40	64.0
5_1^-	4558	90.2	4.84	20.4
4_2^-	6143	23.0	5.43	2.7
4_3^-	8370	45.1	5.14	1.7
4_5^-	8903	55.0	5.05	1.5

TABLE X. ^{34}Si electromagnetic transition strengths connecting the lowest-lying 0^+, 3^-, 4^-, and 5^- states. The units of $B(\lambda)$ are μ_N^2 fm^{2L-2} and e^2fm^{2L} for ML and EL transitions, respectively. The corresponding single-particle (Weisskopf) units for M1, E2, E3, and M4 transitions in ^{34}Si are 1.791 μ_N^2, 6.54 e^{2}fm^4, 68.7 e^{2}fm^6, and 2018 μ_N^2fm^6, respectively.

Transition	Multipole (λ)	$B(\lambda)$[a]
$4^-\rightarrow 3^-$	M1	0.44
$5^-\rightarrow 4^-$	M1	0.26
	E2	29.8
$5^-\rightarrow 3^-$	E2	0.002
$3^-\rightarrow 0^+$	E3	51.7(31.4)
$4^-\rightarrow 0^+$	M4	4368(2660)

[a]M1 and E2 $B(\lambda)$ were calculated using the effective (sd) shell operators (see text). B(E3) corresponds to $e_p=1.5e$, $e_n=0.5e$, and B(M4) to the free nucleon g operators. For the E3 and M4 cases, the numbers in parentheses use the effective (sd) operators for E2 and M1 transitions, respectively.

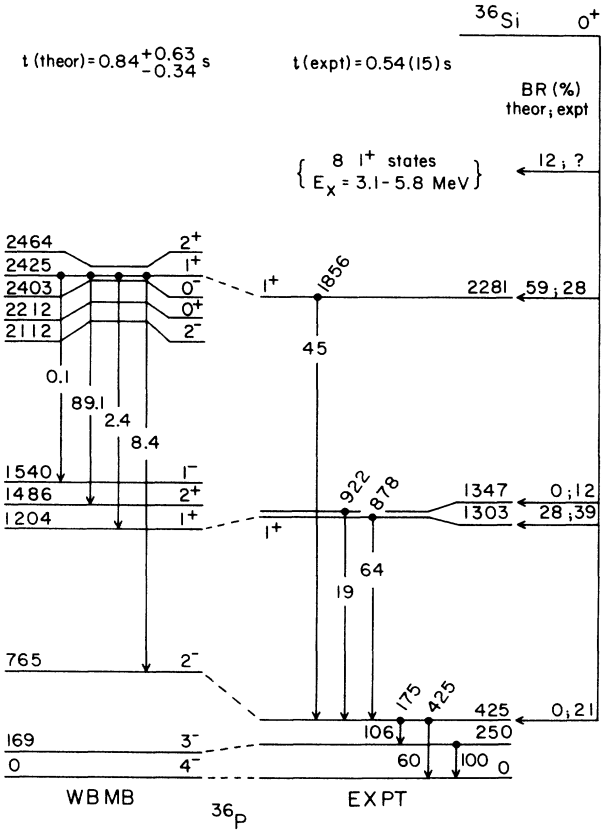

FIG. 2. On the right is shown the proposed decay scheme of ^{36}Si as deduced from the β^--delayed γ-ray spectrum of Dufour *et al.* (Ref. 2). These published results consist of the six γ transitions with their energies given in keV above the transitions and their relative intensities given within the transitions. The β^- branching ratios (BR) we infer from the intensities are given to the far right where they are compared to the WBMB predictions (Table XI). On the left is shown the WBMB energy spectrum for $E_x<2.5$ MeV (one 5^- level is omitted). Also shown are the predicted γ-branching ratios (in percent) of the 1_2^+ state. The uncertainty assigned to the theoretical half-life is due to that in the mass of ^{36}Si.

tremely large strength of the $E2$ decay, the kinematics favor the $M1$ branch which is predicted to be 97%. The 2_1^+ state is predicted to have branching ratios to the 2_1^- and 3_1^- states of 40% and 60%, respectively. Thus, a 1_1^- assignment to the 1347-keV level would give better agreement of the predictions with experiment than would a 2_1^+ assignment.

For either a 1_1^- or 2_1^+ assignment to the 1347-keV level, the observed intensity (12%) of the 922-keV γ transition needs to be explained by γ transitions from higher-lying levels. This is also true for the extra flux (21%) out of the 425-keV level. Thus, even the 12% β^- intensity we predict for levels in the 3.1–5.8 MeV range of excitation is not adequate to explain the extra 33% β^- flux out the 425- and 1347-keV levels. We are led to propose the possibility of an overlooked 934-keV $2281\rightarrow 1347$ γ branch. The γ-ray transition strengths necessary to check whether the WBMB predictions for the decay of 1_2^+ are consistent with this proposal are collected in Table XII and the resulting branching ratios (in

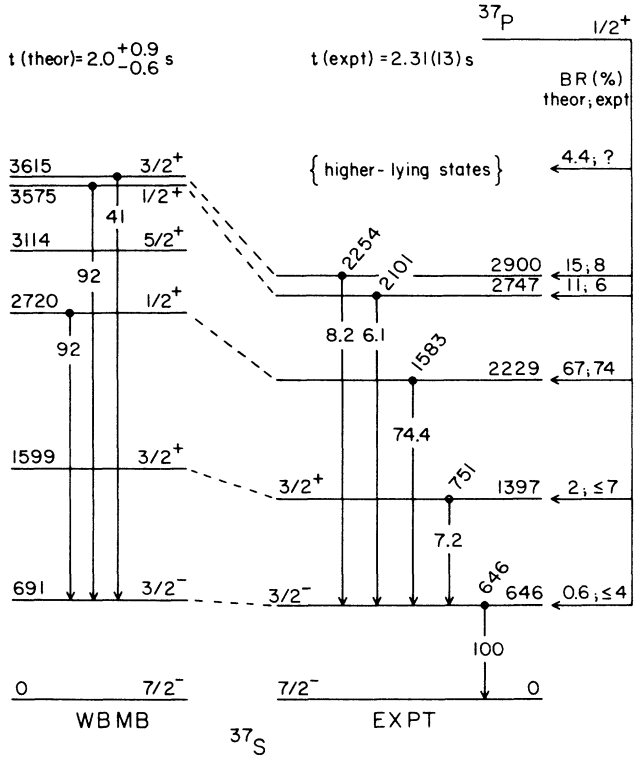

FIG. 3. On the right is shown the proposed decay scheme of ^{37}P as deduced from the β^--delayed γ-ray spectrum of Dufour *et al.* (Ref. 2). These published results consist of the five γ transitions with their energies given in keV above the transitions and their relative intensities given within the transitions. The β^- branching ratios (BR) we infer from these intensities are given to the far right where they are compared to the WBMB predictions (Table XIII). Only states pertinent to the β^- decay are shown. On the left is shown the partial WBMB energy spectrum (only $J^\pi\leq 5/2^+$ levels are shown for $E_x>2.5$ MeV). The uncertainty assigned to the theoretical half-life is due to that in the mass of ^{37}P.

TABLE XI. WBMB description of ^{36}Si(β^-)^{36}P. The predicted half-life is $0.84^{+0.63}_{-0.34}$ s where the uncertainty is due to that in the mass of ^{36}Si. Only 1^+ ^{36}P states for which the branching is $>1\%$ are listed.

J^π_k	E_x (WBMB) (keV)	E_x(expt)[a]	B(GT) ($\times 10^3$)	logft	Branching (%)
2^-_1	765	425		$f=10$	9×10^{-2}
1^+_1	1204	1303	127	4.69	28.3
1^-_1	1540	(1347)[b]		$f=0.4$	7×10^{-3}
1^+_2	2425	2281	599	4.01	59.1
1^+_3	3140		224	4.44	8.7
1^+_4	3482		97	4.80	2.4
1^+_5	3838		73	4.92	1.3
Total					99.9

[a]When listed, the E_x(expt) were used in the calculation of f. For the remaining levels f was calculated using E_x(WBMB).
[b]Uncertain assignment.

TABLE XII. Predicted electromagnetic decays of ^{36}P 1^+ states. The transition strength $B(\lambda)$ is in units of μ_N^2 for M1 transitions and e^2fm^{2L} for EL transitions. Numbers in parentheses are powers of 10.

E_i (keV)	J^π_k Initial	Final	λ	$B(\lambda)$[a]	E_γ (keV)	Γ_γ (meV)	BR[b] (%)
1303	1^+_1	2^-_1	E1	3.82(−6)	878	8.87(−3)	100
2281	1^+_2	2^-_1	E1	5.84(−6)	1856	3.91(−2)	8.4
	1^+_2	1^+_1	M1	2.38(−4)	978	2.58(−3)	2.4
			E2	1.21(+1)	978	8.72(−3)	
	1^+_2	(2^+_1)	M1	4.24(−2)	934[c]	4.01(−1)	89.1
			E2	2.65(+1)	934[c]	1.52(−2)	
	1^+_2	(1^-_1)	E1	4.36(−7)	934[c]	3.72(−4)	0.1

[a]For ^{36}P, single particle (Weisskopf unit) values for the $B(\lambda)$ are 0.703, 7.061, and 1.791 for E1, E2, and M1 transitions, respectively.
[b]γ-ray branching ratio.
[c]Assuming the final state is at 1347 keV.

TABLE XIII. WBMB description of ^{37}P(β^-)^{37}S. The predicted half-life is $2.0^{+0.9}_{-0.6}$ s where the uncertainty is due to that in the mass of ^{37}P. Only even-parity ^{37}S states for which the branching is $>1\%$ are listed.

J^π_k	E_x(WBMB) (keV)	E_x(expt)[a] (keV)	B(GT) ($\times 10^3$)	logft	Branching (%)
$3/2^-_1$	691	646		$f=3.3$	0.12
$3/2^+_1$	1599	1397	3	6.28	2.0
$1/2^-_1$	2360	2638		$f=2.2$	8.2×10^{-2}
$1/2^+_1$	2720	2229	214	4.46	67.3
$1/2^+_2$	3575	2747	55	5.05	10.8
$3/2^+_2$	3615	2900	90	4.84	15.3
$3/2^+_6$	4820		33	5.27	1.2
Total					96.8

[a]When listed the E_x(expt) were used in the calculation of f. For the remaining levels f was calculated using E_x(WBMB).

TABLE XIV. Predicted electromagnetic decays of ^{37}S $1/2^+$ and $3/2^+$ states. The transition strength $B(\lambda)$ is in units of μ_N^2 for M1 transitions and $e^2\text{fm}^{2L}$ for EL transitions. Numbers in parentheses are powers of 10.

E_i (keV)	J_k^π Initial	Final	λ	$B(\lambda)$[a]	E_γ (keV)	Γ_γ (meV)	BR[b] (%)
1397	$3/2_1^+$	$3/2_1^-$	E1	4.89(−7)	751	3.03(−4)	100
2229	$1/2_1^+$	$3/2_1^-$	E1	2.13(−4)	1583	8.85(−1)	92
	$1/2_1^+$	$3/2_1^+$	M1	9.75(−3)	832	6.49(−2)	8
			E2	4.36(+1)		1.40(−2)	
2747	$1/2_2^+$	$3/2_1^-$	E1	8.37(−4)	2101	1.18(+1)	92
2747	$1/2_2^+$	$3/2_1^+$	M1	3.74(−2)	1350	1.06(+0)	8
			E2	2.50(+0)		9.03(−3)	
2900	$3/2_2^+$	$3/2_1^-$	E1	1.52(−5)	2254	1.82(−1)	41
2900	$3/2_2^+$	$3/2_1^+$	M1	5.11(−3)	1503	2.00(−1)	58
			E2	9.33(+0)		5.75(−2)	
2900	$3/2_2^+$	$1/2_1^+$	M1	3.11(−4)	671	1.09(−3)	1
			E2	1.64(+1)		1.80(−3)	

[a]For ^{37}S, single particle (Weisskopf unit) values for the $B(\lambda)$ are 0.717, 7.324, and 1.791 for E1, E2 and M1 transitions, respectively.
[b]γ-ray branching ratios.

percent) are shown in the WBMB predictions of Fig. 2. Clearly the predictions are in disagreement with experiment. For instance, we predict a $1_2^+ \rightarrow 2_1^+$ branch ~ 10 times stronger than the $1_2^+ \rightarrow 2_1^-$ branch we associate with the 1856-keV γ rays. We note, however, that as discussed in Sec. II, the predicted $E1$ transition strengths are subject to larger uncertainties than, say $M1$ strengths. Nevertheless, the predictions for γ-ray decays discussed here suggest the possibility of ambiguities in the singles β^--delayed γ-ray spectrum; i.e., the predicted γ-ray transition energies are such as to suggest an unusually high probability for γ-ray energy doublets in the 900–950 keV range as well as the usual probability of overlooking weak transitions.

In conclusion, we predict the ^{36}Si β^- decay is mainly to the first two 1^+ states. When these states are placed as shown in Fig. 2, we obtain a β^- half-life in agreement with experiment. We view our predictions for $E1$ decays as unreliable, and the experimental γ-ray results as only partially understood, i.e., there are obvious disagreements of the predictions with experiment.

3. $^{37}P(\beta^-)^{37}S$

^{37}P decay was calculated initially with the experimental $Q(\beta^-)$ value, 7587(400) keV, and the ^{37}S spectrum of Table V. With that result as orientation, the level scheme of Fig. 3 was constructed from the five β^--delayed γ rays reported by Dufour *et al.*[2] In doing so we relied on the predicted γ-ray transition strengths and the fact that first-forbidden decay is, once again, of no real importance at the present level of experimental sensitivity. In Table XIII we give the β^- decay results recalculated using the proposed decay scheme of Fig. 3. Predicted γ-ray transition strengths pertinent to the proposed decay scheme are listed in Table XIV. The predicted γ branchings of the $1/2_1^+$, $1/2_2^+$, and $3/2_2^+$ states are of particular interest. For the $1/2^+$ states the dominant branch (92% in each case) is predicted to be to $3/2_1^-$ and thus agrees with the proposed decay scheme on the right of Fig. 3. For the γ decay of $3/2_2^+$ we have a mild disagreement in that the branch to $3/2_1^-$ is predicted to be 41% with a 58% 1503-keV branch to $3/2_1^+$ at 1397 keV. This latter transition was not observed. We have shown the experimental branching ratios into the 646- and 1397-keV levels as limits because the excess γ-ray flux out of these levels could very well be due to γ-ray cascades from higher-lying levels such as the $2900 \rightarrow 1397$ transition just discussed. Given this interpretation, the WBMB predictions are in very good quantitative agreement with the proposed scheme.

IV. DISCUSSION

The present results join previous ones[4,5] in which a good account is given of allowed transitions between $(2s,1d)^n(fp)$ states[1,2] in neutron-rich $A \lesssim 40$ nuclei. We believe that use of the extremely successful USD $(2s,1d)$ interaction is the principal reason for this success. We have concentrated on the β^- decay of $N=21$ and 22 isotones. The daughters have $Z<20$ and the smaller Z is the more that the $1fp$ or $2fp$ states in the daughter nu-

cleus are dominated by neutron, as opposed to proton, excitations to the (fp) shell. Thus, the allowed β^- decays, being $\nu \rightarrow \pi$, are dominated by $(s,d) \rightarrow (s,d)$ transitions with the (fp) or $(fp)^2$ neutrons as spectators. In the present cases, for instance, the contributions from $\nu(fp) \rightarrow \pi(fp)$ transitions are all but negligible. Thus, the success of our calculations of Gamow-Teller transition rates in the present three cases and for ^{37}S, ^{38}Cl (Ref. 4) and ^{35}Si, ^{36}P (Ref. 5) serve to illustrate the validity of the USD interaction outside the range in which it was heretofore tested. As a corollary of these arguments, we note that the dominance of $(s,d) \rightarrow (s,d)$ transitions justifies our use of the effective Gamow-Teller operator extracted from consideration of Gamow-Teller transitions between (sd) shell nuclei (Ref. 13).

ACKNOWLEDGMENTS

Research supported by the U.S. Department of Energy under Contracts No. DE-AC02-76CH00016 (Brookhaven National Laboratory) and No. W-7405-Eng-48 with the University of California (Lawrence Livermore National Laboratory). Computational work was done on computers of the Lawrence Livermore National Laboratory Nuclear Chemistry Division. Special thanks are due to D. R. Manatt for his continued assistance with computer operations.

[1]M. Langevin, E. Quiniou, M. Bernas, J. Galin, J. C. Jacmart, F. Naulin, F. Pougheon, R. Anne, C. Détraz, D. Guerreau, D. Guillemaud-Mueller, and A. C. Mueller, Phys. Lett. **150B**, 71 (1985); D. Guillemaud-Mueller, A. C. Mueller, D. Guerreau, F. Pougheon, R. Anne, M. Bernas, J. Galin, J. C. Macmart, M. Langevin, F. Naulin, E. Quiniou, and C. Détraz, Z. Phys. A **322**, 415 (1985).

[2]J. P. Dufour, R. Del Moral, A. Fleury, E. Hubert, D. Jean, M. S. Pravikoff, H. Delagrange, H. Geissel, and K.-H. Schmidt, Z. Phys. A **324**, 487 (1986). It should be emphasized that this is a preliminary report and the data will almost certainly be revised somewhat before decay schemes are published.

[3]B. H. Wildenthal, M. S. Curtin, and B. A. Brown, Phys. Rev. C **28**, 1343 (1983).

[4]E. K. Warburton, D. E. Alburger, J. A. Becker, B. A. Brown, and S. Raman, Phys. Rev. C **34**, 1031 (1986).

[5]E. K. Warburton and J. A. Becker, Phys. Rev. C **35**, 1851 (1987).

[6]E. K. Warburton, Phys. Rev. C **36**, 2278 (1987).

[7]B. H. Wildenthal, Prog. Part. Nucl. Phys. **11**, 5 (1984).

[8]A comprehensive report of results of the USD interaction (Ref. 7) has not as yet been published. However, a summary of binding energies for $A = 17-39$ has been privately circulated by B. H. Wildenthal.

[9]D. J. Millener and D. Kurath, Nucl. Phys. **A255**, 315 (1975).

[10]J. B. McGrory, Phys. Rev. C **8**, 693 (1973).

[11]B. A. Brown, A. Etchegoyen, W. D. M. Rae, and N. S. Godwin, OXBASH, 1984 (unpublished).

[12]D. H. Gloeckner and R. D. Lawson, Phys. Lett. **53B**, 313 (1974).

[13]D. H. Wilkinson and B. E. F. Macefield, Nucl. Phys. **A232**, 58 (1974).

[14]B. A. Brown and B. H. Wildenthal, At. Data Nucl. Tables **33**, 347 (1985).

[15]The meaning of weak, medium, and strong transition strengths is relative to the mean strength for a particular multipolarity. From Ref. 16, the logarithmic mean strengths for isospin allowed $E1$, $E2$, $E3$, $M1$, and $M2$ transitions in $A = 4-44$ nuclei are about 5×10^{-3}, 4, 10, 0.1, and 0.3 W.u., respectively.

[16]P. M. Endt, At. Data Nucl. Data Tables **23**, 3 (1979).

[17]D. J. Vieira, J. W. Wouters, K. Vaziri, R. H. Kraus, H. Wollnik, G. W. Butler, F. K. Wohn, and A. H. Wapstra, Phys. Rev. Lett. **57**, 3253 (1986).

[18]W. A. Mayer, W. Henning, R. Holzworth, G. Korschinek, W. V. Mayer, G. Rosner, and H. J. Scheerer, Z. Phys. A **319**, 287 (1984).

[19]L. K. Fifield, C. L. Woods, R. A. Bark, P. V. Drumm, and M. A. C. Hotchkis, Nucl. Phys. **440**, 531 (1985).

[20]R. J. Smith, P. J. Woods, R. Chapman, J. L. Durell, J. N. Mo, B. R. Fulton, and R. A. Cunningham, Z. Phys. A **324**, 283 (1986).

[21]P. V. Drumm, L. K. Fifield, R. A. Bark, M. A. C. Hotchkis, and C. L. Woods, Nucl. Phys. **A441**, 95 (1985).

[22]A. H. Wapstra and G. Audi, Nucl. Phys. **A432**, 1 (1985).

[23]G. J. L. Nooren and C. van der Leun, Nucl. Phys. **A423**, 197 (1984); G. J. L. Nooren, H. P. L. de Esch, and C. van der Leun, *ibid.* **A423**, 228 (1984).

[24]S. Piskoř, P. Franc, J. Křeménk, and W. Schäferlingová, Nucl. Phys. **A414**, 219 (1984).

[25]C. E. Thorn, J. W. Olness, E. K. Warburton, and S. Raman, Phys. Rev. C **30**, 1442 (1984).

[26]S. Raman, W. Ratynski, E. T. Jurney, M. E. Bunker, and J. W. Starner, Phys. Rev. C **30**, 26 (1984).

[27]F. Ajzenberg-Selove and G. Igo, Nucl. Phys. **A142**, 641 (1970).

[28]C. L. Woods, Nucl. Phys. **A451**, 413 (1986).

[29]R. K. Bansal and J. B. French, Phys. Lett. **11**, 145 (1965).

[30]B. H. Wildenthal, private communication; see Ref. 4 for details.